Chapter 2

Background

This section presents the this is short and needs a lot more detail and also figures.

This section briefly reviews the current techniques for lung perfusion and hemodynamic monitoring, and provides a general overview of the state of 3D EIT as used for thoracic imaging and monitoring.

2.1 Impedance Imaging

Impedance imaging has been in use since the early 1900s for geophisical applications. Originally introduced as a technique to image below the earth's surface, current was transmitted between two electrodes placed into the ground and any anomalies in subsurface conductivity produced deviation in the equipotential lines. Including current injections and measurements from multiple locations and using known electrical properties of geological structures Conrad Schlumberger identified features of underground geological structures (Allaud and Martin, 1977).

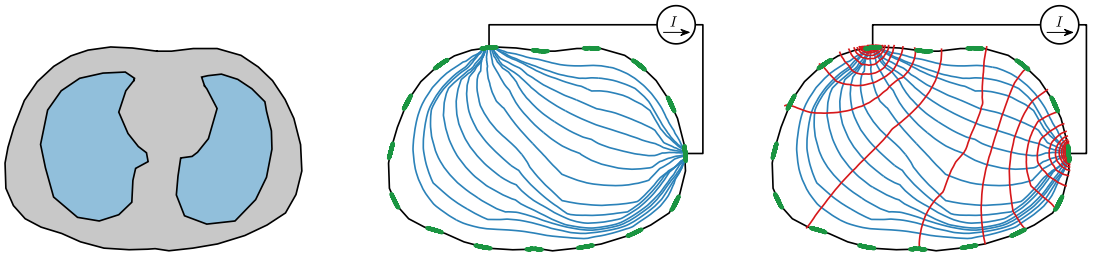

Figure 2.1: (A) A body comprising tissues of different conductivity, (B) Electrodes are placed on the surface and current is injected between a pair or electrodes. The current pathways are indicated by the blue lines. (C) The resulting equipotential lines within the body are shown in red.

These same techniques can be applied in biomedical applications where voltage is measured on an array of body surface electrodes while current is applied between select electrode pairs (figure 2.1). Due to impedance differences associated with biological tissues and their physiological function (**Geddes1967**; **McAdams1995**), EIT has been proposed for a wide range of applications from thoracic monitoring to neuronal and brain imaging (**Holder1992**; **Frerichs2016**).

2.2 Bioimpedance

In thoracic imaging the most commonly measured impedance changes occur due to movement of air in the lungs, the flow of blood, and the motion of organs (Adler and Boyle, 2017). During inhalation, the volume of air in the lungs increases, lowering the conductivity of the lung tissue. The resistivity of lung tissue varies significantly between expiration and inspiration giving a value of 7 Ω m during expiration and 23

Ω m during inspiration at 100 kHz (Witsoe and Kinnen, 1967), resulting in a measureable variation in impednace during respiration (Eyüboğlu *et al.*, 1989). There are also other signifant sources of impedance change that make EIT signal intrepretation challenging. Simulations have attributed up to 20 percent of the respiratory signal to the effect of chest expansion and movement of the chest wall (Adler *et al.*, 1994).

The source of impedance changes due to the flow of blood is even more complex. Since the resistivity of blood is so much lower than other tissues (1.5 Ω m), the increase of blood due to pulsatile flow should decrease the impecance of structures it passes through by a detectable amount (Eyüboğlu *et al.*, 1989). It is often assumed that the component of EIT images at the cardiac frequency is related to the perfusion of blood, but the exact source of cardiosynchronus EIT signals is unclear (Nguyen *et al.*, 2012; Patterson, 2010). A continuous flow of blood alone is insufficient to induce a significant impednce change, as the volume and concentration of the conductive medium is unchanged. Any impedance-based measure of perfusion relies on the cardiosynchronous EIT signals which have numerous possible sources (Adler *et al.*, 2017b).

2.2.1 The Cardiac Cycle

The cardiac cycle consists of the activity in the heart between the beginning of one heart beat, and the next. There are two main stages of the cardiac cycle: the diastole, when the heart relaxes and is filled with blood, and the systole, when contraction of the heart pumps blood to lungs and all other body systems (Pappano and Wier,

2019). A simplified anatomy of the heart is presented in figure 2.2. Since ECG recordings are frequently used to synchronize EIT data, it is helpful to look at the timing of the cardiac cycle as it relates to features of ECG traces. An example ECG waveform is pictured in figure 2.3.

During the first stage of the cardiac cycle is the ventricular diastole, indicated by the P wave on an ECG trace, during which the heart relaxes and expands pulling blood into the ventricles from the atria (Pappano and Wier, 2019). Blood enters the atrium on the right side of the heart through the superior and inferior vena cava and on the left side of the heart, the atrium is filled by oxygenated blood from the lungs through the pulmonary veins (Pappano and Wier, 2019). Next is the atrial contraction during which time the atria pump additional blood into the ventricles, and the ventricular volume and pressure is maximized. At the peak of the ventricular volume, the ventricles contract and depolarize which corresponds to the QRS complex (Pollock and Makaryus, 2021). On the right side of the heart, deoxygenated blood is pumped to the lungs where it perfuses into the lung tissue, and on the left side of the heart oxygenated blood is pumped to the rest of the body through the aorta (Pappano and Wier, 2019). The smallest volume in the ventricles occurs after the ventricular repolarization represented in the ECG by T wave (Pollock and Makaryus, 2021).

2.2.2 Bioimpedance of Perfusion

There are several factors that may contribute some part of the impedance change during the cardiac cycle. Some of these factors include:

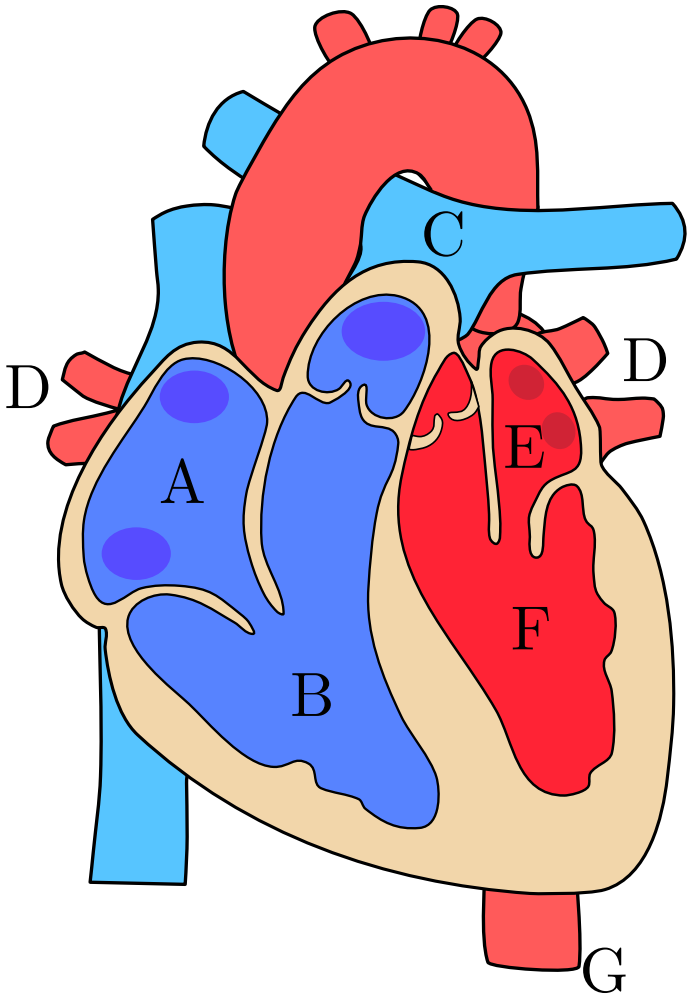

Figure 2.2: The pathway of the blood from entry to the heart to the descending aorta is indicated by the letters. Deoxygenated blood enters the heart through the right atrium (A) where it is moved to the right ventricle (B). From there it passes through the pulmonary artery (C) into the lungs where it perfuses and is oxygenated. Blood return from the lungs through the pulmonary veins (D) then enters the left atrium (E). Finally, the blood is pumped from the left ventricle (F) to the rest of the body through the aorta, and the descending aorta (G).

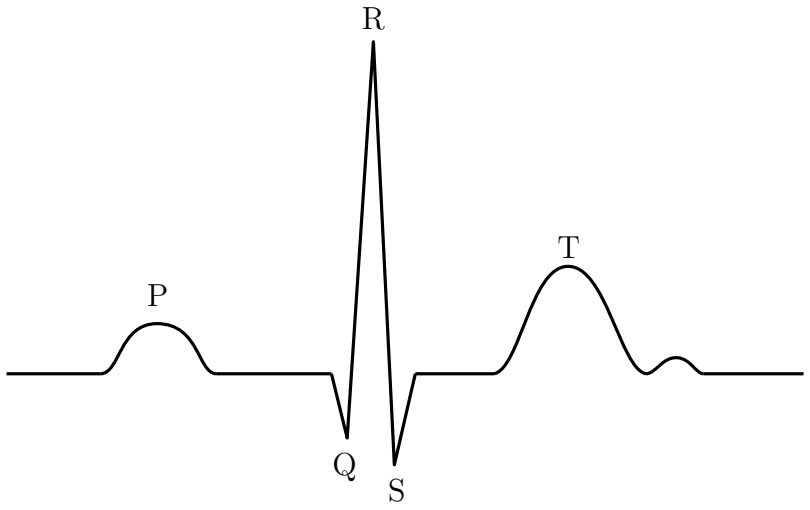

Figure 2.3: An example ECG waveform to compare electrical signals in the heart to blood volume changes. The P wave represents the beginning of the cardiac cycle with the ventricles begin to fill. The QRS complex corresponds with ventricular depolarization and occurs as the ventricles contract they contract. The beginning of the QRS complex corresponds with the maximum ventricular volume. The minimum volume in the ventricles occurs after ventricular repolarization represented by the T wave.

- Changes in blood volume within the heart as blood is pumped. As the ventricles fill with blood the volume increases and results in a more conductive heart (Nyboer *et al.*, 1970).
- Variations in arterial and blood vessel volume. Due to the elasticity of arteries and blood vessels, the pulsatile flow of blood passing through results in variation of vessel diameter, affecting the impedance (Eyüboğlu *et al.*, 1987).
- Physical deformation of structures due to motion of the heart. The motion of the heart can have significant contribution to cardiosynchronous EIT images (Adler *et al.*, 2017b; Proença *et al.*, 2015), with simulations showing that heart motion was the main contributor to impedance change due to the ventricle (Proença *et al.*, 2015).

- The orientation of red blood cells. During pulsatile flow the orientation of red blood cells changes, which had been shown to affect the impedance of the blood (Gaw, 2010).
- Ballistic forces in the body generated by the heart. During each heartbeat blood is pumped downwards through the descending aorta with a large force pushing the rest of the body upwards (Gordon, 1877). Different directions of flow in the aorta result in a repeating ballistic signal on the rest of the body (Kim *et al.*, 2016). This results in motion on the electrodes and body which can introduce significant artefacts in EIT signals (Adler *et al.*, 1994).

The contribution of each of these factors will ultimately depend on the placement of the electrodes and the specific geometry and physiology of a patient. When imaging changes in stroke volume, changes relating to posture, breathing and changes in belt position resulted in changes that overpowers the perfusion signals (Patterson *et al.*, 2001).

Despite the challenges of isolating cardiosynchronous EIT signals related to perfusion there is still a great interest in improving accuracy and stability due to the unique advantages offered by EIT over current state-of-the-art methods.

2.3 Perfusion Imaging

Determining the flow of blod within vital organs such as the heart, brain and lungs allows doctors to make quivk dicieiosn to treat patients in life threatning situations. In the braing perfusion imaging can be used to diagnose and monitoor dementia

and Alzheimer's disease (Barker *et al.*, 2014; Dougall *et al.*, 2004), or to detect and diagnose ischemic strokes (Koenig *et al.*, 1998; Konstas *et al.*, 2009). Perfusion images of the heart can be used to diagnose ischemic heart disease (Prvulovich and Bomanji, 1998), which is caused by a reduction of blood flow to the heart, typically due to a build-up of plaque in the arteris of the heart (Mendis *et al.*, 2011). Ventilation/perfusion scans can be used in the lungs to measure the distribution of perfusion and ventilation in the lungs (Mortensen and Berg, 2019). The primary use is to detect mismatches between the ventilation in perfusion to detect pulmonay embolysms (PIOPED-Investigators, 1990).

Nuclear medicine has been at the forefrtont of perufsion imaging, but has a long acquisition time, and images can be fuzzy and challenging to intrepret (). Recent developments in CT and MRI imaging yeild clearer images and can give metrics regarding blood flow and blood volume over a period of time (Prvulovich and Bomanji, 1998). EIT has been proposed as a technique to monitor perfusion due to its sensitivity to blood movment, and development is currently underway to establish EIT as a technique to monitor perfusion (Nguyen *et al.*, 2015; Nguyen *et al.*, 2012), blood flow (Braun *et al.*, 2018a; Braun *et al.*, 2018b), and blood pressure (Proença *et al.*, 2020; Proença *et al.*, 2017). The following section explores the advantages and pitfalls of state of the art perfusion monitoring techniques.

2.3.1 Nuclear Medical Imagaing

The two primary nuclear medicine techniques used for perfusion imagaing are single-photon emission computed tomography (SPECT), and scrintigraphy. These tech-

niques image gamma rays that are emitted from a gamma-emitting radionuclidite injected into the patient (Mettler and Guiberteau, 2006). The radioisotopes are integrated into drugs that enable them to travel to a specific organ or tissue. Perfusion imaging with scintigraphy and SPECT is primarily used in the lungs and heart. The emitted gamma rays are measured by external detectors called gamma cameras (Mettler and Guiberteau, 2006). The main difference between the two is that SPECT creates 3D images, and scintigraphy images are 2D. Scintigraphy uses a gamma camera place in a single location, while SPECT uses a detector that roates around the patient and captures gamma images from several angles. A typical SPECT system rotates 3–5 degrees per acquisiton and takes apprximately 15–20 minutes to complete a full scan, although scan times can be shorter when multiple detectors are used to capture images from multiple angles simultaneously (Mettler and Guiberteau, 2006).

TODO: THIS IS HARD

Ventilation/perfusiuon scans area a specefic type of perfusion sacn that uses lung scintigraphy. During ventilation an aresolized radionuclitide is inhaled through a mask placed over the nose and mouth. To image lung perfusion the radionuclitide is injected and its passage through the lung is imaged. Both phases are imaged using a gamma camera (Mortensen and Berg, 2019). This technique can be time and labour intensive, and results in radiation exposure to both the technitian and patient (Gandev *et al.*, 2005). The duration of a single scan to measure ventilation and perfusion is approximately 15 minutes, including time time required to breath the radionuclidite prior to imaging (Hur *et al.*, 2014). Reducing the time required to reduce radiation exposure has been shown to give less reliable measures of perfusion

(Hur *et al.*, 2014). Despite the widespread clinical use to diagnose

2.3.2 CT

2.3.3 MRI

2.3.4 EIT

EIT has been suggested as an ideal tool to continuously monitor perfusion (Leonhardt and Lachmann, 2012). EIT is cost-effective, non-invasive, does not use ionizing radiation, and images can be acquired contiunuoisly at a high sampleing rate (Adler and Boyle, 2017). Despite these advantages of EIT, spatial resolution is low, and image accuracy is further limited by artefacts introducted by poor electrode contact and electrode movement (Adler and Boyle, 2017). The spatial resolution of EIT is typically thought to be approximately 20–50% of the electrode seperation, but can be afectetd by the measurement protocol and image reconstruction techniques (Polydorides and McCann, 2002).

EIT has been evaluated for its ability to measure cardiac output and lung perfusion since the late 1980s (Brown *et al.*, 1992; Eyüboğlu *et al.*, 1989; Frerichs *et al.*, 2002; Zadehkoochak *et al.*, 1992). Since then, various configurations of EIT have been evaluated (Borges *et al.*, 2012; Nguyen *et al.*, 2015). Due to the speed and safety of measurement acquisition, EIT might be used to continuously monitor perfusion in subjects mush more frequently than current state of the art techniques.

There are two main ways perfusion related changes can be imaged with EIT. Like with many perfusion imaging techniques, a contrast agent can be injected to image

the transit of blood through vessels and organs. Typically a sodium chloride bolus with a concentration between 5–20% is used as a contrast agent for EIT (Nguyen *et al.*, 2012), and an algorithm to determine the regional blood flow to the lung and heart (Borges *et al.*, 2012). This technique was found that measures of perfusion using a contrast agent with EIT were highly correlated to SPECT images of perfusion (Borges *et al.*, 2012). The same study found that pulsatile images of EIT showed little correlation to bolus measures and SPECT scans.

When breathing is paused, the signals based only on the cardiac activity can be more easily extracted. It was found that during apnoea the global impedance recorded with EIT measurements corresponded with stroke volume measured using the thermodilution method with a pulmonary arterial catheter (**Fagerberg2009**). Ventilation perfusion ratios have been calculated during apnoea by comparing ventilation and perfusion signal amplitude with a specified region of interest (**Fagerberg2009a**). There is some concern that the perfusion measured during apnoea may not accurately represent true perfusion during regular respiration as the apnoea impacts the regular respiratory cycle (Leonhardt and Lachmann, 2012), and since apnoea cannot be sustained continuously there is interest in an alternative method to increase sensitivity to cardiosynchronous changes.

The majority of work on perfusion imagingin with EIT has focused on imaging the pulsatile or cardiosynchronous component of EIT data (Nguyen *et al.*, 2012). As discussed in section section 2.2.2 there are many potential sources of the cardiosynchronous signal, and the effect of perfusion related changes is not well understood. Perfusion had been calculated using digital filtering to extract the related

componenet of an EIT signal. Deibele *et al.* (2008) have shown that principal component analysis (PCA) can be used to separate ventilation and cardiac frequency signals and identify the component related to the heart. Once the cardiac-frequency component of the EIT signal is identified the pulmonary component must also be isolated. One of the most widely used techniques is selecting a region of interest that corresponds to the organ, tissue or flow to me measured (Braun *et al.*, 2018a; Solà *et al.*, 2011).

Techniques to improve accuracy of EIT models and increase sensitivity to cardiosynchronous activity such as internal and 3D electrode configurations could improve accuracy of techniques to isolate pulsatile activitiy in a specific region, and could enable an improved perfusion measure using EIT, and a means of continuously monitoring perfusion during ventilation. In this thesis we explore the effect of both increased mesh accuracy and internal electrodes, and discuss their potential for improving sensitivity to perfusion with EIT.

2.4 Electrical Impedance Tomography

Most EIT systems consist of: a current source to inject a current between two electrodes; a system to measure differential voltage between pairs of electrodes; and electrodes, applied to the body surface. This section further discsses each of these aspects of EIT and introduces concepts of image acquisition and reconstruction

2.4.1 EIT measurements

A "frame" of EIT data consists of a series of measurements made on an array of electrodes placed around a region of interest. In this thesis we focus on measurements of the thorax.

2.4.1.1 Electrodes

EIT recordings are made using several types of electrodes. Both polarizable and non-polarizable electrode types are used, silver-silver chloride electrodes are often applied directly to the body and stainless steel, brass, textile and rubber electrodes have also been used (Adler and Boyle, 2017) and are sometimes integrated into electrode belts. The polarization of EIT electrodes is not significant at the frequencies (>20 kHz) that are typically used (Adler and Boyle, 2017).

When making measurements with EIT systems there is very little current flowing through non-injecting electrodes due to the high impedance of the integrated voltmeter (Holder, 2004). For this reason, the effects of the electrode-body impedance are minimal on electrodes that are not injecting current. Measurements that are

largely affected by this impedance on injecting electrodes typically have a phase shift and are often removed before reconstruction.

Changing contact impedance has a large effect on EIT measurements can be influenced by changes in posture or pressure on electrodes (Coulombe *et al.*, 2005). Contact impedance is often improved on electrodes by adding a conductive gel (Waldmann *et al.*, 2017), but it can decrease over long measurements as the gel dries (Lozano *et al.*, 1995).

2.4.1.2 Current injection and voltage measurement

To calculate impedance three main conisderations must be made with regard to the injected current: the frequency, amplitude and pattern.

Low frequency currents will prefferentially pass around cells through the extracellular fluid due to the high capacitive componenet of the cell membrane (Foster and Lukaski, 1996), wheras high frequency currents will be more affected by the capacitive componenet (Holder, 2004). Since EIT requires a linear relationship between the measured voltages and tissue impedance to produce valid reconstructions, it is important to select frequencies of less than 1 MHz to ensure that cell and neural membrane is not the dominant factor in the impedance measurements (Barber and Brown, 1984). Impedance measurements below 100 KHz have shown to be primarily rsitive on lung tissue (Witsoe and Kinnen, 1967), and most EIT systems use frequencies between 10 kHz and 1 Mhz (Holder, 2004).

The selection of current amplitudes is primarily selected based on considerations to patient safety (Adler and Boyle, 2017). The guideline defined by IEC 60601-1

(International Electrotechnical Commission, 2021), set a limit of 10 mA on current across all electrodes at 100 kHz, and lower limits at lower frequencies. For EIT frequencies between 20–100 kHz are often used with an injected current between 1–5 mA. In order to meet the guidelines at low frequencies, when injecting sinusoidal currents it is also important to use complete current cycles so that DC currents are not applied to the body (Adler and Boyle, 2017). When using internal electrodes there are additional safety considerations that limit current amplitudes

The pattern of current injection and voltage measurement is commonly refered to in EIT as the stimulation and measuremnt pattern. Typically a current is injected between two electrodes while the resulting voltages are measured between asjacent pairs. The two most common injection patterns are adjacent, and "skip 4". Examples of these measurement patterns are shown in figure 2.4 on a 16 electrode system. The terms adjacent and skip 4 describe the space between pairs of injecting or measurement electrodes. Regardless of the pattern, a frame of EIT data is generated in the same way. Current is injected between a pair of electrodes as voltage is measured between all remaining pairs, then current is injected between the next pair of electrodes and voltages are measured again. This results in voltage measurements on each electrode pair for every current injection. For a 16 electrode system this results in 256 measurements in each frame. For a 32 electrode system there are 1024. As mentioned in section 2.4.1.1, voltage measurements made on the stimulating electrodes are often removed resulting in 208 measurements per frame on a 16 electrode system, and 928 measurements per frame on a 32 electrode system.

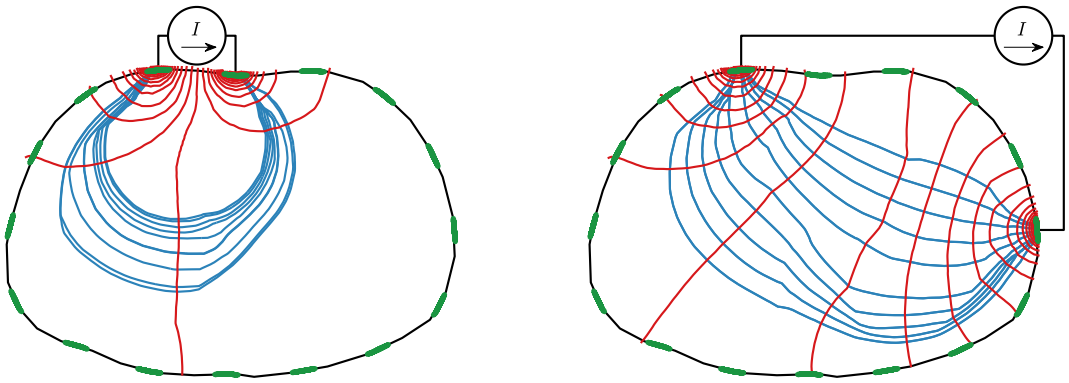

(A) (B)

Figure 2.4: Two common stimulation patterns are simulated on a simple human model showin in figure 2.1. Injected current is shown in blue and the resulting equipotential lines are shown in red. (A) An exmaple of an adjacent stimulation pattern. Current is injected between pairs of adjacent electrodes. For each current injection voltage is measured between all sequential pairs. (B) An example of the "skip 4" injection pattern. Current is injected between every 5^{th} electrode skipping 4 between the injecting electrodes. during each current injection, voltage measurements are made using the same skip 4 pattern between each of the 16 electrodes and their corresponding pair. A single frame of data is generated by all measurements made for each possible injection pattern. For 16 electrodes this results in 256 meaasurements.

2.4.2 Imaging Techniques

There are several challenges that make absolute EIT imaging difficult. The differences in tissue impedance are subtle relative to artefact introduced by unknown boundary locations and electrode positions (Adler and Boyle, 2017; Adler *et al.*, 2015; Nissinen *et al.*, 2009). EIT is instead typically used to reconstruct impedance changes between two points in time.

Time difference EIT is sensitive to the movement of fluis within the body and is well suited to image functional activity such as the inflation of the lungs and the flow of blood. Time-difference EIT is also much more stable in the presence of errors that remain constant such as incorrectly modelled boundary and electrode locations (Adler and Boyle, 2017; Brown, 2003). Frequency difference EIT is also possible based on the different impedance response of tissue types to changing frequencies. Frequency difference uses two or more different frequencies and calculates an image based on the change in electrical properties. Most frequencies used to differentiate between different tissue types are at high frequencies where current starts to flow across the cell membranes. These high frequencies are out of the range of most current EIT systems and frequency changes due to different lower frequencies are limited (Adler and Boyle, 2017). This thesis uses time-difference EIT to images changes in movemnt and fluid volumes in teh thorax.

2.4.3 Forward Problem

In simulation, we have a model with known geometry and impedance and we wish to solve for the voltage at the electrodes due to a stimulation current. This process

is called the forward problem. A model used to calculate a solution for the forward problem is called a forward model.

This problem is well-posed, and can be solved analytically on simple, regular geometries. For the inverse solution we require Maxwell's forumlation of Faraday's Law:

$$\Delta \times \vec{E} = -\frac{\partial}{\partial t}\vec{B} \tag{2.1}$$

and Ampere's Law:

$$\Delta \times \vec{H} = \vec{J} + \frac{\partial}{\partial t}\vec{D}. \tag{2.2}$$

To set up the solution we first assume that the current used for EIT is sufficiently low frequency relative to the scale of interest that we can use a quasistatic approximation of Maxwell's equations (Larsson, 2007). Under this assumption the derivitave components of equation (2.1) and equation (2.2) can be set to zero giving:

$$\Delta \times \vec{E} = 0 \tag{2.3}$$

and

$$\Delta \times \vec{H} = \vec{J}. \tag{2.4}$$

In this static case the electric field due to a potential can be described by

$$\vec{E} = -\Delta\vec{u}. \tag{2.5}$$

Finally we require Ohm's Law, describing the relationship between the current

density, conductivity and electric field:

$$\vec{J} = \sigma \vec{E}. \tag{2.6}$$

Using the magnetic field identity for the divergence of curl $\Delta \cdot (\Delta \times \vec{H}) = 0$ with equation (2.4), we get

$$\Delta \cdot \vec{J} = 0. \tag{2.7}$$

Combining equation (2.7) with Ohm's Law (equation (2.6)) we get

$$\Delta \cdot (\sigma \vec{E}) = 0. \tag{2.8}$$

And finally with equation (2.5) relating the electric field and potential we get

$$\Delta \cdot \sigma \Delta \vec{u} = 0 \tag{2.9}$$

which gives the relationship between a conductivity distribution and the resulting potential.

The current density on the boundary is given by:

$$j_n = -\vec{J} \cdot \vec{n} = \sigma \Delta \vec{u} \cdot \vec{n}. \tag{2.10}$$

Where $\vec{n}$ is a unit vector normal to the boundary. Equation (2.10) cannot be used in EIT where the current density on the boundary is not uniform (Somersalo *et al.*, 1992). Instead we require a formulation that give current density on injecting

electrodes and no current density on the rest of the boundary (Somersalo *et al.*, 1992). Somersalo *et al.* (1992) give a formulation of a complete electrode model for the voltage on L electrodes (E) where the voltage measured on each electrode (U) is constant.

$$u + z_l(\sigma \Delta u \cdot \vec{n}) = U_l \qquad \text{on} \quad E_l, \qquad l = 1, 2, \cdots, L. \tag{2.11}$$

The impedance of each electrode contact (z) is also typically trated as a constant over the surface of an electrode (Somersalo *et al.*, 1992). This complete electrode model has been shown to predict voltage accurately (Somersalo *et al.*, 1992).

2.4.4 Discretization and the Finite Element Method

For EIT an analytic soltutions are possible for simple geometires, but in a majority or cases numerical methods are required. One of the primary discritization techniques is the finite element method FEM where the domain is divided into a number of smaller elements. An element is triangular in 2D and tetrehedral in 3D. The collection of nodes, and elements making up a larger model is commonly called a mesh. Each line connecting two nodes of a mesh can be visualized as a resistor, used to model the conductivity of an object.

2.4.5 Inverse Problem

To reconstruct images we must solve for impedance distribution from known voltage measurements. This is known as the inverse problem. The ability to reconstruct impedance distributions from a known voltage distribution is challenging and relies

on the assumption that the relationship between voltage and conductivity is linear (Barber and Brown, 1984). Unlike the forward problem, due to the small number of electrodes relative to the large number of internal elements the inverse probelm is ill-posed (Holder, 2004).

The sensitivity of EIT is often represented by a jacobian matrix, $\mathbf{J}$, which gives the change in measurement relative to another factor. To reconstruct a conductivitiy distribution a conductivity jacobian, $\mathbf{J}_c$, is used which links the change in boundary voltage measurements to the change in impedance. It can be represented by

$$\mathbf{J}_C = \frac{\Delta U}{\Delta \sigma}. \tag{2.12}$$

The jacobian gives the relationship between the conductivity of each voxel, and the resulting measurements (Holder, 2004). In practice the jacobian can be calculated using the adjoint field (Vauhkonen *et al.*, 1999).

2.4.5.1 Regularization

The sensitivity of measurements to changes is vastly different throughout the model. Near electrodes where the current density is high, there is high sensitivity to conductivity changes but there is limited sensitivity away from the electrodes. This contributes to the ill-posed nature of the inverse problem (Holder, 2004). To overcome this regularzation must be used to stabalize reconstruction. Regularization imposes restrictions on a minimization problem to ensure a unique solution. In EIT some typical regularization techniques include the maximum *a priori* approach (Adler and Guardo, 1996), Tikhonov regularization (Vauhkonen *et al.*, 1998), and singular value

decomposition (Ostebee, 1998).

2.4.5.2 Image Reconstruction

The standard linear formulation (Holder, 2004) to solve for the conductivity change in each voxel ($\Delta\hat{\sigma}$) for a given set of difference measurements ($\mathbf{b}$) is

$$\Delta\hat{\sigma} = \mathbf{J}^T\mathbf{W}(\mathbf{J}\mathbf{W}\mathbf{J}^T + \mathbf{W})^{-1}\mathbf{b}. \tag{2.13}$$

Where $\mathbf{W}$ is a convariance matrix that incorporates *a priori* information such as the error weighting, and regularization (Adler and Guardo, 1996). The term $\mathbf{J}^T\mathbf{W}(\mathbf{J}\mathbf{W}\mathbf{J}^T + \mathbf{W})^{-1}$ is also called the reconstruction matrix and can be represented by the term $\mathbf{R}$, since after initial calculation it typiclaly remains constant for a given model. Conductivity distributions can be solved using the reconstruction matrix using the equation:

$$\Delta\hat{\sigma} = \mathbf{R}\mathbf{b}. \tag{2.14}$$

There are several techniques used to calculate error weighting and prior information represented by $\mathbf{W}$, such as the NOSER algorithm (Cheney *et al.*, 1990). There are also techniques that have been specifically designed to compentaste for the limitations and characteristics of EIT systems such as GREIT (Adler *et al.*, 2009).

2.4.5.3 Image Reconstruction with GREIT

GREIT (Graz consensus Reconstruction algorithm for EIT) is a consensus algorithm that is used to reconstruct EIT images according to limitations and characteristics of typical EIT systems (Adler *et al.*, 2009). The reconstruction matrix calculated with GREIT depends on the forward model, noise model and the desired performance metrics. GREIT uses a forward model that models electrodes using the complete electrode model discussed in section 2.4.3. The forward model has information regarding the stimulation measurement pattern, body geomerty, and electrodes.

GREIT constructs a set of training images using a small (less than 5% of the model diameter) conductive target in the forward model. A training set consists of images of a conductive object placed at many (100–500) locations within the model. A noise model consisting of of a gaussian estimate of measurement noise, and measurements with electrode motion noise is generated.

Training targets are blurred so that their diameter increases to 20% of the model diameter, but the position remains constant. This is used as the desired image for a training target. The weighting relative to noise and other perfomance metrics is set to minimize recoonstruction errors between the training target and idea image. The weights are set based on the radius of the training image to penalize changes outside the desired image radius to minimize shape deformation and ringing artefact. The weighting can also be adjusted to meet specific perfomance characteristics of interest. A description of all performance characteristics that can be specified is found in (Adler *et al.*, 2009). When applying the training, weighting is also set to increase uniformity of the resolution in the reconstructed image. Some resolution

near the electrode is lost, but weighting help to ensure that targets reconstruct to the same size throught the model.

To calculate a reconstruction martix ()$\mathbb{R}$), error (ϵ) is minimized over all training targets (k) with respect to the weighting parameters ($\mathbf{w}^{(k)}$), measurements ($\mathbf{b}$), and the desired images ($\tilde{\mathbf{x}}$).

$$\epsilon^2 = \sum_k \|\tilde{\mathbf{x}}^{(k)} - \mathbf{R}\mathbf{b}^{(k)}\|^2_{\mathbf{w}^{(k)}} \tag{2.15}$$

To minimize the equation for error we set the derivative of ϵ^2 with respect to the reconstruction matrix equal to 0.

$$\epsilon^2 = \sum_k \|\tilde{\mathbf{x}}^{(k)} - \mathbf{R}\mathbf{b}^{(k)}\|^2_{\mathbf{W}^{(k)}} \tag{2.16}$$

Grychtol *et al.* (2016) show that equation (2.15) can be rearranged to solve for the reconstruction matrix as:

$$\mathbf{R} = \mathbf{D}\mathbf{\Sigma}_t\mathbf{J}^T(\mathbf{J}\mathbf{\Sigma}_t\mathbf{J}^T + \Lambda\mathbf{\Sigma}_n)^{-1} \tag{2.17}$$

Where $\mathbf{D}$ is the desired image matric from all training images, $\mathbf{\Sigma}_t$ is the effective covariance of all training targets after weighting with $\mathbf{W}$ and $\mathbf{\Sigma}_n$ is thr noise covarience. This reconstruciton method is widely used in EIT for both 2D and 3D electrode configurations and is shown to give even resolution throughout the image (Adler *et al.*, 2009).

2.4.6 Internal Electrodes

TODO: ADD overview from whereever I put it!

2.4.6.1 Motion Correction

TODO: Just background

2.5 Summary

TODO: bring it back to the general motivation briefly